20th International Conference on Renewable Energies and Power Quality (ICREPQ'22)
Vigo (Spain), 27th to 29th July 2022
Renewable Energy and Power Quality Journal (RE&PQJ)
ISSN 2172-038 X, Volume No.20, September 2022

Design of a water channel to model the wave conditions in the Colombian Pacific Ocean

Rubio-Clemente A[1,2], Velásquez L[1], Chica E[1]

[1] Grupo de Investigación Energía Alternativa, Facultad de Ingeniería, Universidad de Antioquia UdeA, Calle 70, No. 52-21, Medellín, Colombia.

[2] Escuela Ambiental, Facultad de Ingeniería, Universidad de Antioquia UdeA, Calle 70, No. 52-21, Medellín, Colombia.

Phone/Fax number: 0057(4)3405555, e-mail: ainhoa.rubioc@udea.edu.co

Abstract. During the design process of an efficient wave energy converter (WEC), a crucial aspect is its performance evaluation in wave channels able to generate dynamic waves simulating the ocean conditions. This work presents the design of a water channel that simulates the wave conditions of the Pacific Ocean in Colombia. The designed channel has a rectangular cross-section with width, length and depth equal to 0.49 m, 7.35 m and 1.47 m, respectively. In the channel, the steepness ratio can vary from 0.0134 to 0.544 for a wavelength of 1.47 m. Additionally, the channel was computationally modelled in order to know the behaviour of the waves generated. In this regard, an efficient WEC able to take profit of the Colombia's capacity for producing electricity from waves is feasible, contributing to the reduction of greenhouse gases and, therefore, to sustainable development.

Key words. Wave energy, hydrodynamic modelling, wave channel

1. Introduction

At present, several potential renewable energy resources such as ocean and tidal currents, salinity gradient, thermal energy and waves, are derived from seawater. Among them, wave power has a worldwide theoretical potential estimated in 29500 TWh/year. For an appropriate use of this available resource, several wave energy converters (WECs) have been developed to take profit of the wave energy. WECs capture kinetic and potential energy from waves to transform them into electricity [1]-[3].

Nowadays, WECs have several stages of development and they are the subject of investigation around the world [4, 5]. As a matter of fact, a number of studies in the literature have been focused in the WEC design optimization, as well as in the control strategy methodologies to increase the WEC performance. The most common types of WECs that can be distinguished are attenuators, overtopping, oscillating water column, oscillating body systems and point absorbers, which are characterized by the way they interact with ocean waves [5]. The WECs must be weather resistant during their life time and economically attractive; therefore, their conversion efficiency and the investment costs must be high and low, respectively. Additionally, WECs can be used as floating or fixed structures in offshore areas or located along the coastlines, respectively. The design and selection of the WECs depend on the particular location physical characteristics and the wave conditions (i.e., the wave direction, height (H) and period (T)). In this regard, the characterization of the wave conditions from the potential sites where the WECs will be installed is of utmost importance [6]. This aspect allows to improve the WECs due to the wave conditions at the operation site greatly affect their performance. For this purpose, having experimental facilities that enable the design and development of these new technologies is required to convert the energy available in waves into electricity [4]-[6].

In Colombia, the renewable electricity is gaining an increased interest. In this context, wave energy is an available and predictable resource with limited environmental impacts that can provide part of the country electricity demand [5]-[8]. However, this resource is still unexplored and several devices to convert wave energy into electricity must be further improved or developed for the local ocean conditions to efficiently transform the wave energy and become the WECs economically competitive in comparison with other more mature renewable technologies [9].

Concerning the wave resource evaluation in Colombia, from the authors' knowledge, several works reported in the literature are highlighted. Among them, the study developed by Restrepo and López analyzed the variability of the waves and the morphology of the main deltas along the Colombian Caribbean Sea and Pacific Ocean [10]. In turn, Portilla and co-workers researched the wave conditions at 4 locations in the Colombian Pacific Ocean [11]. Osorio et al. estimated the available energy potential in the Caribbean Sea and the Pacific Ocean of Colombia [9, 12], and found that for the Caribbean Sea regardless of the presence of El Niño or La Niña phenomena, the most energetic waves were observed during the months of December, January and February. In the case of the Caribbean Sea, the highest values of mean wave power were around 5-7 kW/m and

appeared from December to February, coinciding with one of the windy summer seasons in Colombia. This period also match with the least rainy period in the country; period in which the water level of rivers and reservoirs decreases. On the contrary, during the winter season, the average wave power barely reached 1 kW/m. In the case of the Colombian Pacific Coast, the maximum power of the waves has been observed to be close to half of the energy potential estimated in the Caribbean Sea (i.e., around 2-3 kW/m) throughout the year, except the quarter that goes from June to August, when the resource of the waves is less abundant [9, 12].

It is important to note that the wave energy potential of Colombia is low when compared to other places around the world. However, this available resource could be used to complement the national energy system, especially in the summer months when there is less rain causing less capacity of hydroelectric power generation due to the low levels of rivers and water reservoirs. When this happens, thermal plants complement the energy generation system, causing a rise in electricity prices and an increase in greenhouse gas emissions. The wave energy potential could also be used to supply non-interconnected areas in the country. In the case of the complementarity of the Colombian energy system with plants that take advantage of wave energy, these should be installed near urban centers with availability of a distribution network.

Unfortunately, according to the best knowledge of the authors, a channel designed for the wave conditions in the Colombian Pacific Ocean has not been reported in the scientific literature yet.

Under this scenario, the aim of this work is to design a wave channel able to model regular wave trains in deep and intermediate water with similar characteristics as the Colombia Pacific Ocean conditions to create innovative and reliable WECs locally that transform the wave energy into useful energy.

2. Wave channel design

2.1 Description of the wave channel

A wave channel is a tank with a length much greater than the width and height. As recommended in the literature, a large tank width should not be considered so that frictional effects are negligible. On the other hand, the tank height should be that one for the desired wave to be produced.

The channel has three perfectly differentiated zones, including the wave generation, propagation and extinction zones [13]. The generation zone is located at one of the ends of the channel, where the wave formation occurs. The main components of this zone are the generator or wave maker, the power system and the control system. In the literature, three types of wave makers are normally presented; the flap-type (waves are produced by flap oscillation), the plunger-type (the wave is produced when the wave maker vertically oscillates throughout the surface of water), the piston-type (a movable wall generates the waves by an oscillatory motion in the wave propagation direction) and the rotor-type (a blade is located on the rotor surface, so that when the rotor begins to rotate, the blade displaces the water volume in order to produce the wave) [13]. All the wave maker types have advantages and limitations. In this regard, the flap-type can be used for the wave generation from deep water, while the piston-type wave maker is able to short wave production, and the rotor-type can generate a high torque even with a low rotation velocity (rpm). In turn, the plunger-type wave maker is generally in shape of wedge and it can easily located within the channel [14]-[16]. In Fig. 1, these types of wave makers are illustrated.

The wave generation process begins by entering into the control system the parameters controlling the wave maker movement, such as the blade stroke, and the velocity and the acceleration-deceleration, by which the generator movement is described. The period at which the generation system is moved will correspond to the period of the generated wave [15].

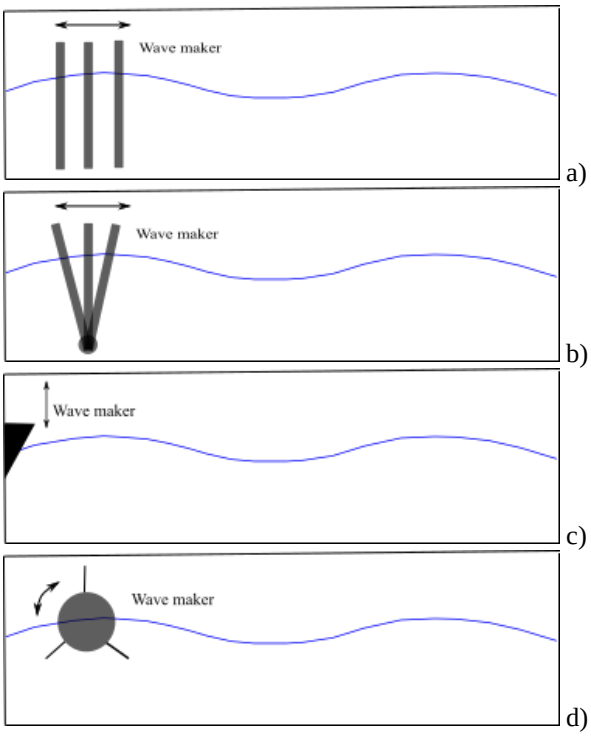

Fig. 1. Types of wave makers. a) piston-type wave maker, b) flap-type wave maker, c) rotor-type wave maker, d) plunger-type wave maker.

In turn, the propagation zone is the longest section of the channel due to the produced wave in the generation zone must be properly developed, for which space is required. For obtaining a fully developed wave, the propagation zone length is estimated to be at least twice the generated wave length. Finally, the extinction zone corresponds to the end of the channel, which is located opposite the wave generation zone [17]. There are basically two types of absorption systems: active and passive ones. The active systems work with control algorithms that make the generator movement to be modified as a function of the height of the wave reaching it [17]. In contrast, the passive systems consist of structures acting as the beach;

in fact, they usually receive this name when they are composed of porous beds containing rocks or stones. When no absorbent system is placed, the waves would bounce off the channel wall, being reflected almost completely, and hindering the development of the incident waves [17, 18]. The geometric configuration of the passive absorption elements can be diverse and their design will largely be dependent on the study to be conducted. The most typical wave absorbers are inclined planes, vertical mesh and porous parabolas. For a beach to achieve a good energy dissipation, a gentle slope of ~ 1:10 is needed. The general principles of the wave absorbers are based on the wave energy dissipation due to the wave breaking caused by the water depth (d) reduction. Usually, when the ratio of the wave height (H) to the wavelength (L) is equal to 1/7 and H is equal or higher than three-fourths of d, the waves begin to break [13, 17, 18].

Generally, when carrying out studies based on harnessing the wave energy, the goal is to dissipate most of the energy contained in the waves passing through the device in question, so they do not bounce. Therefore, absorption devices consist of a ramp resting on the channel bottom, which acts as a beach [17]. On the surface, stones or other elements acting as obstacles to the wave can be placed. When the wave hits the obstacle, most of the wave energy is absorbed. Nevertheless, a small amount of this energy is not dissipated, being reflected and travelling in the opposite direction to the waves produced through the generator [17, 18].

In turn, the tank length should be at least four times the wavelength for the waves to be propagated before they reach the beach, which is located at the tank end, allowing a full development of the waves so that the secondary waves existing near the wave maker do not be considered in the area of study. A long tank also allows the correction of abnormalities ascribed to the wave motion [16].

2.2 Wave characteristics

Before beginning with the design of a wave channel, examining the profiles of the waves existing in nature is required in order to decide which ones of these profiles are going to be reproduced in miniature in the wave channel. In this work, a wave channel was designed for simulating the hydrodynamics and the geometric conditions of the Colombian Pacific Ocean waves. The main parameters describing the waves are L, H, T and d, over which the waves are propagated. Fig. 2 illustrates a schema of wave propagation in the X direction *versus* time (t).

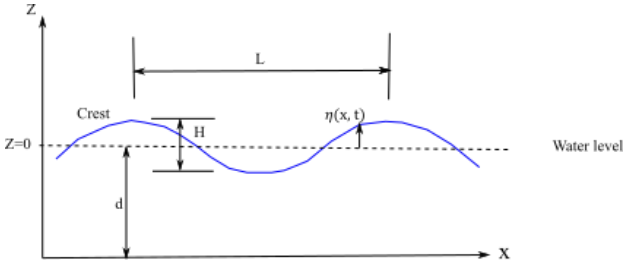

Fig. 2 Wave characteristics

L is related to d and T, and refers to the horizontal distance between two successive wave crests. The wave velocity, also well-known as celerity (C), is defined as the distance travelled by the wave in a time T; i.e., it refers to L/T ratio [19, 20]. The waves can be classified on the basis of T, as follows: capillary waves (T < 0.1 s), ultra-gravity waves (0.1 s < T < 1 s), ordinary gravity waves (1 s < T < 30 s), infra-gravity waves (30 s < T < 5 min), long-period waves (5 min < T < 12 h), ordinary waves (12 h < T < 24 h) and trans-tidal waves (T > 24 h). Other way for waves to be classified is focusing on the L/d ratio. Whether the value of L/d is small (L/d ≤ 2), the wave is a deep-water wave. For intermediate or transitional-water waves, L/d is between 2 and 20 (2 < L/d < 20). On the other hand, when L/d is large (L/d ≥ 20), the wave is a shallow-water wave. Another significant physical feature of waves is the steepness (σ). This parameter is equal to H/L ratio. Waves have a limiting value of σ, beyond which they start to break. This situation occurs when the centripetal acceleration of the water particles at the crest is equal to the acceleration due to gravity (g). σ and the ratio L/h are the factors used in establishing the geometric similitudes between natural waves and the laboratory-scaled waves [13].

Table I. Linear-wave and second-order Stokes theory equations

Linear-wave theory			
Water depth/wavelength (d/L)	Shallow water d/L<1/20	Transitional water 1/20<d/L<1/2	Deep water d/L>1/2
Wave profile (η)	$\eta = \frac{H}{2}\mathrm{Cos}\left[\frac{2\pi x}{L} - \frac{2\pi t}{T}\right]$		
Wave celerity (C)	$C = \sqrt{gd}$	$C = \sqrt{\frac{gL}{2\pi}\mathrm{Tanh}\left(\frac{2\pi d}{L}\right)}$	$C = \sqrt{\frac{gL}{2\pi}}$
Wavelength (L)	$L = T\sqrt{gd}$	$L = \frac{gT^2}{2\pi}\mathrm{Tanh}\left(\frac{2\pi d}{L}\right)$	$L = \frac{gT^2}{2\pi}$
Second-order Stokes theory			
Water depth/wavelength (d/L)	Transitional water 1/20<d/L<1/2		
Wave profile (η)	$\eta = \frac{H}{2}\mathrm{Cos}\left[\frac{2\pi x}{L} - \frac{2\pi t}{T}\right] + \frac{\pi H^2}{2L}\frac{\mathrm{Cosh}\left(\frac{2\pi}{L}d\right)\left[2+\mathrm{Cosh}\left(\frac{4\pi}{L}d\right)\right]}{\left(\mathrm{Sinh}\left(\frac{2\pi}{L}d\right)\right)^3}\mathrm{Cos}\left[\frac{2\pi x}{L} - \frac{2\pi t}{T}\right]$		
Wave celerity (C)	$C = \sqrt{\frac{gL}{2\pi}\mathrm{Tanh}\left(\frac{2\pi d}{L}\right)}$		
Wavelength (L)	$L = \frac{gT^2}{2\pi}\mathrm{Tanh}\left(\frac{2\pi d}{L}\right)$		
η, is a harmonic function describing the surface elevation of a regular wave.			

For energy generation, the deep and intermediate water waves are very important since the energy available is higher in comparison with that one in shallow water waves [13].

Several mathematical theories describing the behaviour of gravity waves in water have been developed, being the linear-wave theory (Airy theory) or the first-order Stokes theory widely used [19, 20]. Le Méhauté proposed qualitative criteria to determine the most appropriate theory for describing each particular wave based on T, H and d presented in a dimensionless form [13, 21].

Using the second-order Stokes theory and the linear-wave theory, the wave characteristics shown in Table I can be determined. For the design of the wave channel, the conditions of the waves generated in the Colombian Pacific Ocean previously reported from buoys moored near the edge of the continental shelf at Tumaco, Gorgona Island, Buenaventura Harbour and Solano Bay locations were used as shown in Fig. 3 [11]. The wave characteristics are listed in Table II.

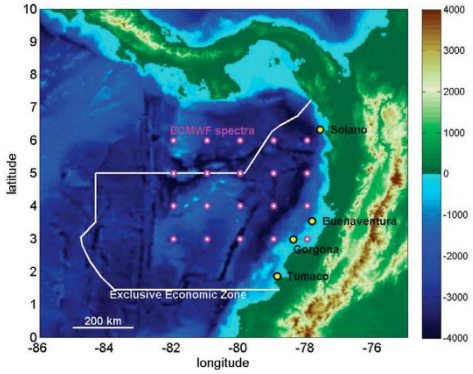

Fig. 3. The study area in the Colombian Pacific Ocean [11]

Using the diagram provided by Le Méhauté shown in Fig. 4, the most suitable wave theory was selected for analysing the wave conditions from the Colombian Pacific Ocean. For using this diagram, knowing d, T and H of the study zone is required. With the relationships of $d/(gT^2)$ and $H/(gT^2)$ axes, several points were obtained and placed on the diagram. From Fig. 4 and the represented points, the most adequate wave theory to be used for the theoretical calculations can be identified. To plot the red parallelogram depicted in Fig. 4, the pairs of points (d_{min}, H_{min}-T_{max}; d_{min}, H_{max}, T_{max}; d_{max},, H_{max}-T_{min}; and d_{max}, H_{min}-T_{min}) were used from the data set listed in Table II. The max and min subscripts represent the maximum and the minimum values, respectively, of the aforementioned variables. The red zone represents the limit states of the sea that can occur in the specified area of study. In turn, Fig. 4 shows that the linear theory for intermediate and deep water is adequate to represent the data set.

Table II. Data of the waves generated in the Colombian Pacific Ocean [11]

Location	Wave height mean (H, m)	Wave period mean (T, s)	Mooring water depth (d, m)
Tumaco	1.01	6.86	146
Gorgona Island	1.13	7.76	135
Buenaventura Harbour	0.96	8.21	150
Solano Bay	1.17	10.61	130

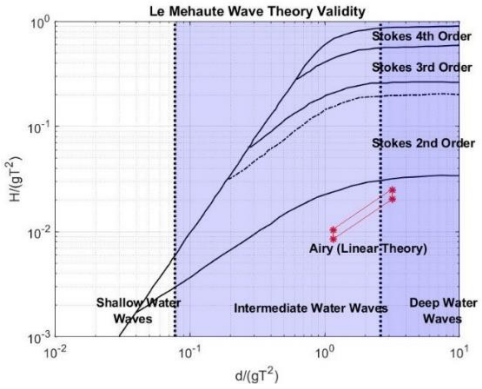

Fig. 4. Diagram of Le Méhauté considering the wave conditions of the Colombian Pacific Ocean

2.3 Design of the wave tank

Because of the ocean size and depth with respect to the size of the channel wave, an adequate scaling must be carried out. In this regard, dynamic and kinematic similarities must exist between the waves generated in nature and those ones produced in the prototyped wave channel so that experimental results can be scaled [11, 21]. For this purpose, the forces influencing the fluid dynamics must be considered, being the viscosity, gravity, pressure, surface tension and elasticity the most important ones in hydraulic studies. These forces are non-dimensionally represented by considering the ratio of the forces to the resultant inertia force, leading to the Reynolds (Re), Froude (Fr), Strouhal (St), Euler (Eu), Weber and Cauchy numbers. It is important to note that the Weber and Cauchy numbers can be neglected in water waves, since they are very small. Nonetheless, the Re and Fr numbers must be taken into account during the water wave scaling. In turn, the number representing the pressure forces (Eu number) will be automatically satisfied whether the other dimensionless numbers are accomplished [22]. With regard to the primary types of waves generated in a wave channel (that is, the gravity waves), the gravity and inertial forces are the main forces produced. On the other hand, the ratio of the inertial force to the pressure force or gravity (Fr number) can be considered in the scaling practice when viscous effects are negligible. Fr is expressed as Eq. (1) [23, 24].

$$F_r = \frac{\rho V^2}{\rho g d} = \frac{V^2}{g d} \tag{1}$$

where V is the velocity of the fluid, ρ refers to the density of the sea water (here, ρ is equal to 1025 kg/m^3), and g stands for the gravity acceleration (i.e., 9.81 m/s^2). Froude scaling assumes Fr as a constant value between the model and the full-scale (Eq. (2)), resulting in $\boldsymbol{\lambda}$ (Eq. (3)), expressing the geometric scale, being p and m the prototype and the model, respectively [23]-[25].

$$\left.\frac{V^2}{gd}\right|_p = \left.\frac{V^2}{gd}\right|_m \tag{2}$$

$$\lambda = \left(\frac{V_m}{V_p}\right)^2 = \frac{d_m}{d_p} \tag{3}$$

The velocity ratio is, therefore, $\lambda^{1/2}$, and the geometric scales or distance ratio is λ. The ratio for the time scale is also $\lambda^{1/2}$, following the relationship shown in Eq. (4) [23, 24].

$$\frac{T_m}{T_p} = \frac{L_m/V_m}{L_p/V_p} = \left(\frac{L_m}{L_p}\right)\left(\frac{V_p}{V_m}\right) = \lambda\left(\frac{1}{\lambda^{1/2}}\right) = \lambda^{1/2} \quad (4)$$

The methodology used in the scaling process ensures that the Fr, St and Eu numbers obtained in the Colombian Pacific Ocean are equal to those ones achieved in the wave tank [23]-[25].

To calculate the wave L, Eq. (5) and (6) were used for intermediate and deep water, respectively.

$$L = \frac{gT^2}{2\pi} Tanh\left(\frac{2\pi d}{L}\right) \quad (5)$$

$$L = \frac{gT^2}{2\pi} \quad (6)$$

For the design of the wave channel, the limit values were analysed, which coincided with the pairs: i) d_{min}, H_{min}-T_{max}, ii) d_{min}, H_{max}, T_{max}, iii) d_{max},, H_{max}-T_{min}, and iv) d_{max}, H_{min}-T_{min}. Due to Eq. (5) is an implicit equation as far as the variable L is concerned, it must be solved by iteration. The results obtained for L are presented in Table III.

Table III. Determination of the wavelength (L)

Setting	D (m)	H (m)	T (s)	L (m) for intermediate water	L (m) for deep water
d_{min}, H_{min}-T_{max}	130	0.96	10.61	175.73	176.76
d_{min}, H_{max}, T_{max}	130	1.17	10.61	175.73	175.76
d_{max},, H_{max}-T_{min}	150	1.17	6.86	73.47	73.47
d_{max}, H_{min}-T_{min}.	150	0.96	6.86	73.47	73.47

Generally, the parameters concerning waves, including H, T and L, are used to define the wave conditions to be reproduced in the channel at a fixed scale. A scaling factor λ equal to 50 was selected for simulated the wave characteristics in the wave tanks [25]. In Table IV, the wave characteristics for the Colombian Pacific Ocean and the wave tank are presented.

Table IV. Dynamically scaled wave characteristics

	H (m)	T (s)	L (m)
Wave Ocean condition (d_{min}, H_{min}-T_{max})	0.96	10.61	175.73
Wave tank condition	0.02	1.50	3.52
Wave Ocean condition (d_{min}, H_{max}, T_{max})	1.17	10.61	175.73
Wave tank condition	0.02	1.50	3.52
Wave Ocean condition (d_{max},, H_{max}-T_{min})	1.17	6.86	73.47
Wave tank condition	0.02	0.97	1.47
Wave Ocean condition (d_{max}, H_{min}-T_{min}.)	0.96	6.86	73.47
Wave tank condition	0.02	0.97	1.47

Due to the space limitations in the laboratory where the channel will be installed, the maximum value of L that can be reproduced in the channel was defined to be equal to 1.47 m. The dimensions of the channel listed in Fig. 5 were defined in terms of L. For the channel width, a value of L/3 can be used to guarantee the generation of wave trains in two-dimensions. The flap was located at a distance equal to L from one side of the channel.

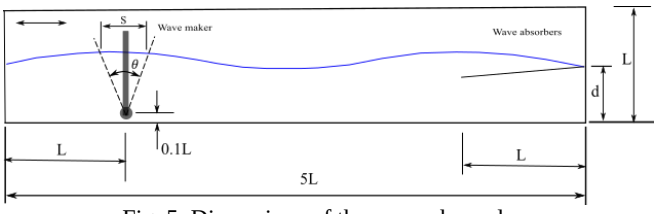

Fig. 5. Dimensions of the wave channel

A flap-type wave maker was selected for the wave channel design. The flap frequency was assumed to be that one of the produced waves. Therefore, by using Eq. (7), the H of the target wave can be related to the stroke of the flap (S) [25].

$$\frac{H}{S} = 4\left(\frac{Sinh\,(kd)}{kd}\right)\left(\frac{khSinh(kd) - \cosh(kd) + 1}{Sinh\,(2kd) + 2kd}\right) \quad (7)$$

Using Eq. (7) and considering a specific relative water depth (kd) value, the S required for obtaining a desired H can be achieved, being k the wave number, which is equal to 2π/L. The flap angular motion can be defined as a function of the control system quality. A suggested value of the flap displacement angle is between -12° and +12°. As a recommendation, the flap should be extended ~ 35% of the hinge depth above the waterline. In order to calculate S, a range of d between 0.1 m and 0.8 m was established for H between 0.02 m and 0.1 m. The values of S for the wave channel are compiled in Table V. The maximum strokes (S_{max}) for the flap are also presented in Table V for the different depths to which it could operate on the wave channel.

In Table V, the values shaded in red are those ones that cannot be given due to the S_{max} restrictions of the flap system. The flap used for the design of the wave channel was a plate, which is hinged on a sill at 0.1 L of distance above the wave channel bottom. The flap dimensions were established as L/3-2gap, 1.35d and 6.35 mm (1/4 in) of width, height and thickness, respectively. When installed in the tank, a gap of 2 mm along each side is maintained. The flap motion will be driven by an electric servo drive motor.

Table V. Maximum stroke values (S_{max}) for a wavelength equal to 1.47 m

L=1.47 m									
H (m)	d (m)	0.8	0.7	0.6	0.5	0.4	0.3	0.2	0.1
0.10	S (m)	0.070	0.074	0.081	0.091	0.110	0.146	0.224	0.461
0.08		0.056	0.059	0.064	0.073	0.088	0.117	0.179	0.369
0.06		0.042	0.045	0.048	0.055	0.066	0.088	0.134	0.277
0.04		0.028	0.030	0.032	0.036	0.044	0.058	0.089	0.185
0.02		0.014	0.015	0.016	0.018	0.022	0.029	0.045	0.092
S_{max}		0.340	0.298	0.255	0.213	0.170	0.128	0.085	0.043
Flap length		1.080	0.945	0.810	0.675	0.540	0.405	0.270	0.135
T		0.971	0.973	0.976	0.984	1.003	1.048	1.165	1.528

Neglecting friction and mechanical losses, and using the wave maker theory, the power (P) per unit width of the flap is given by Eq. (8) [20, 26]. The maximum value of P that is equal to 22.56 W/m occurs for H and d values of 0.1 m and 0.4 m, respectively.

$$P = 2\frac{\pi\rho g S^2}{kT}\left(\frac{Tanh\,(kd)}{kd}\right)\left(\frac{khSinh(kd) - \cosh(kd) + 1}{Sinh\,(2kd) + 2kd}\right)^2 \quad (8)$$

Finally, for the channel design, a passive absorber type sloping beach that does not reach the bottom of the channel was used in order to minimize wave reflections using minimal space. The advantage of this type of beach is that less material is needed for its manufacture. The slope used for the design was 1:10 at the waterline.

2.4 Numerical simulation of the wave channel

A three-dimensional model of the wave channel design was studied employing a numerical analysis performed in Ansys Fluent software. The dimensions of the computational domain were similar to those ones shown in Fig. 5. A two-phase Eulerian volume of fluid (VoF) was used as a base for the physical model [13], considering an unsteady model, gravity and the SST k-ω turbulence model. The flap cyclic motion is described by a user-defined function, which is based on the flap period and amplitude. The blade movement start to displace the water volume for the wave generation. During the simulation, both the fluid air and water were assumed to be incompressible. The volume fractions of fluids were defined. In this regard, the level of water was established to be equal to 0.8 m. The computational domain was a rectangular region that was discretized using poly-hex core mesh. This domain consists of a stationary and rotational domain. The optimal value of the time step and the number of elements were 0.05 s and 593,143 elements, respectively.

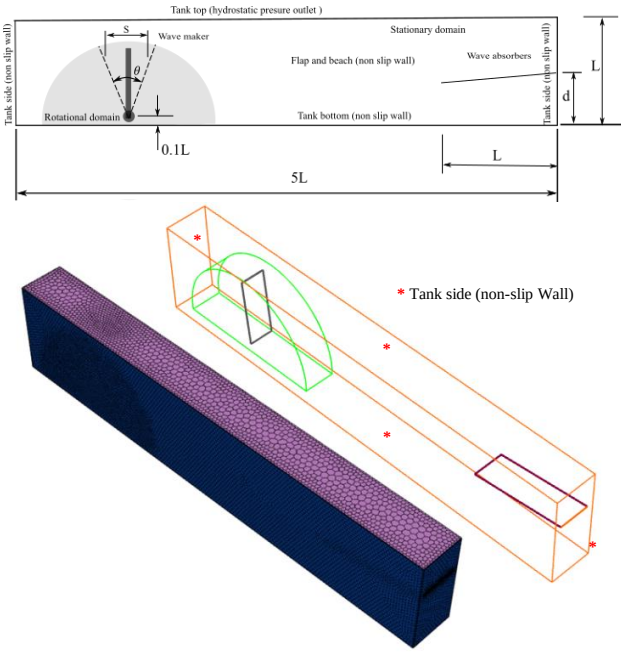

Fig. 6. Computational domain used for the numerical analysis

The boundary conditions represented in Fig. 6, such as the free surfaces and walls, were specified in the numerical analysis. A pressure outlet boundary condition was defined at the domain top boundary. The no-slip boundary condition was imposed on the walls of tank (front, posterior, laterals or tank side and bottom surfaces), flap and beach. Numerical results in terms of the wave crest, trough and mean water level were used to compare against the data of wave conditions in the Colombian Pacific Ocean. In order to get stable time profile of wave quantities, a computational time of 50 s was defined for the simulation. The flap was modelled like an oscillating wall with a stroke equal to 0.07 m.

3. Results and discussion

The designed wave channel had a length, width and depth of 7.35 m, 0.49 m and 1.47 m, respectively. The side walls will be made of glass plates or acrylic sheet to allow a clear view so that the wave characteristics are examined. The wave channel was focused on developing two dimensional wave trains, so that the infrastructure has to be narrow enough to avoid three-dimensional effects. In turn, the length of the channel was long enough to guarantee fully developed waves [27]. During the simulation was identified that the propagation area was approximately between 2.5 to 6.5 m from the left wall of the channel. In this zone, the wave once fully developed travels along the channel without suffering any significant modification on it wavelength, period, height or shape. This is the appropriate zone to carry out experiments with WECs.

In the channel, a flap-type wave maker, which is hinged at the bottom, produces oscillatory, sinusoidal waves. The channel can be operated with a d between 0.1m and 0.8 m, in order to reach values of wave H ranged from 0.02 to 0.10 m, respectively.

Fig. 7 illustrates the wave generation in the channel and its propagation to the right. The volume fraction of water shown in Fig. 7 for the model with and without beach is represented at a time equal to 12 s.

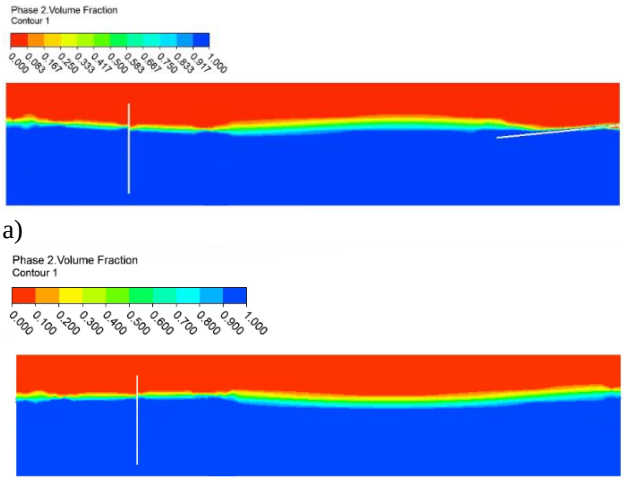

Fig. 7. Volume fraction of the fluid in the wave channel. Numerical model a) with and b) without beach.

A good correlation of the water surface elevation profile and the expected wave H of 0.1 m for the simulated numerical case can be observed in Fig. 8. The beach used in the extinction area enabled the wave energy to be dissipated, reducing the wave reflection considerably. This fact was characterized by the reflection coefficient,

which is the ratio of the reflected wave H to the incident wave H. From the numerical results, the minimum value of the reflection coefficient was 0.12, which implies a significant reduction of the wave energy.

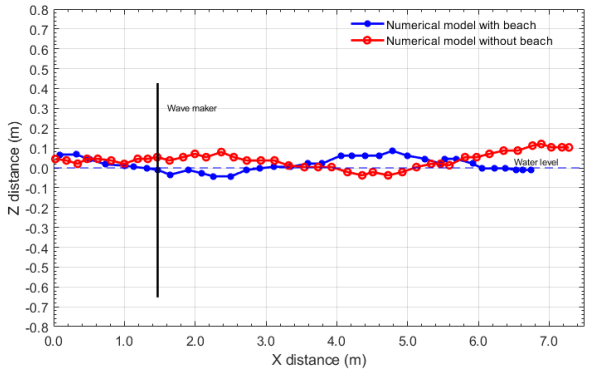

Fig. 8. Water surface elevation

The wave channel designed can be widely used to analyse the behaviour of new WECs at small scale and representative sea conditions, such as those ones of the Pacific Ocean in Colombia because of their relative low cost and great effectiveness.

In order to validate the numeric results and to be able to start with the development of WECs that will take advantage of the energy potential available in the Colombian Pacific Ocean, data published in the literature are required. Nevertheless, as mentioned above, from the authors´ knowledge, designed WECs are not informed in the literature. Therefore, the results obtained from simulation studies cannot be comparable with the scientific literature. This leads to the urgent need of manufacturing this type of wave channels in the country.

4. Conclusion

In this study, a wave channel was designed for testing WECs. The wave tank has been sized based on the dynamic scaling of wave characteristics from the Colombian Pacific Ocean. The selection of the wave tank components and dimensions is dictated by the nature of the wave formed to be simulated. The channel had a tested section measuring in 7.35 m, 0.49 m and 1.47 m (length, wide and depth, respectively), and it can be operated up to a d value of 0.8 m. Different types of waves can be generated by adjusting the water depth, the flap velocity and the stroke length. In the channel, a wave with T, L and H equal to 1.048 s, 1.47 m and 0.1 m, respectively, can be obtained.

From the wave simulation, determining the vertical position of the crests is possible, which allowed to calculate the wave H, and showing a reasonable match to the expected H of 0.1 m.

With the designed WEC, Colombia could take profit of the energy contained in waves, leading to sustainable development achievement.

Acknowledgement

The authors gratefully acknowledge the financial support provided by the announcement No. 890 de 2020 “Convocatoria para el fortalecimiento de CTeI en Instituciones de Educación de Educación Superior (IES) Públicas 2020 (Contract No. 2022-0452). Authors also acknowledge the financial support provided by Universidad de Antioquia (Estrategia de Sostenibilidad 2020-2021. ES84190067).

References

[1] Li, M., Luo, H., Zhou, S., Kumar, G. M. S., Guo, X., Law, T. C., & Cao, S. State-of-the-art review of the flexibility and feasibility of emerging offshore and coastal ocean energy technologies in East and Southeast Asia. Renewable and Sustainable Energy Reviews, (2022), 162, 112404.

[2] Jin, S., and Greaves, D. Wave energy in the UK: Status review and future perspectives. Renewable and Sustainable Energy Reviews, (2021). Vol, 143, pp. 110932.

[3] Aderinto, T., and Li, H. Review on power performance and efficiency of wave energy converters. Energies, (2019). Vol. 12(22), pp. 4329.

[4] Gallutia, D., Fard, M. T., Soto, M. G., & He, J. Recent advances in wave energy conversion systems: From wave theory to devices and control strategies. Ocean Engineering, (2022), Vol. 252, 111105.

[5] Garcia-Teruel, A., and Forehand, D.I.M. A review of geometry optimisation of wave energy converters. Renewable and Sustainable Energy Reviews, (2021). Vol. 139, pp. 110593.

[6] Zhang, Y., Zhao, Y., Sun, W., and Li, J. Ocean wave energy converters: Technical principle, device realization, and performance evaluation. Renewable and Sustainable Energy Reviews, (2021). Vol. 141, pp. 110764.

[7] Ahn, S., Haas, K.A., and Neary, V.S. Wave energy resource characterization and assessment for coastal waters of the United States. Applied Energy, (2020). Vol. 267, pp. 114922.

[8] Weiss, C.V., Guanche, R., Ondiviela, B., Castellanos, O.F., and Juanes, J. Marine renewable energy potential: A global perspective for offshore wind and wave exploitation. Energy Conversion and Management, (2018). Vol. 177, pp. 43-54.

[9] Osorio, A.F., Ortega, S., and Arango-Aramburo, S. Assessment of the marine power potential in Colombia. Renewable and Sustainable Energy Reviews, (2016). Vol. 53, pp. 966-977.

[10] Restrepo, J.D., and López, S. A. Morphodynamics of the Pacific and Caribbean deltas of Colombia, South America. Journal of South American Earth Sciences, (2008). Vol. 25(1), pp. 1–21.

[11] Portilla, J., Caicedo, A.L., Padilla-Hernández, R., and Cavaleri, L. Spectral wave conditions in the Colombian Pacific Ocean. Ocean Modelling, (2015), Vol. 92, pp. 149–168.

[12] Osorio, A.F., Montoya, R.D., Ortiz, J.C., and Peláez, D. Construction of synthetic ocean wave series along the Colombian Caribbean Coast: A wave climate analysis,” Applied Ocean Research, (2016), Vol. 56, pp. 119–131.

[13] Izquierdo, U., Esteban, G.A., Blanco, J.M., Albaina, I., and Peña, A. Experimental validation of a CFD model using a narrow wave flume. Applied Ocean Research, (2019). Vol. 86, pp. 1-12.

[14] Wilkinson, L., Whittaker, T.J.T., Thies, P.R., Day, S., and Ingram, D. The power-capture of a nearshore, modular, flap-type wave energy converter in regular waves. Ocean Engineering, (2017). Vol. 137, pp. 394-403.

[15] Sun, B., Li, C., Yang, S., and Zhang, H. A simplified method and numerical simulation for wedge-shaped plunger wavemaker. Ocean Engineering, (2021). Vol. 241, pp. 110023.
[16] Saha, B., Islam, M., Torab, A., and Ahmed, D.H. (2017). Investigation of wave characteristics with rotor type water wave generator. Journal on Today's Ideas-Tomorrow's Technologies, (2017). Vol. 5(2), pp. 123-140.
[17] Ouellet, Y., and Datta, I. A survey of wave absorbers. Journal of Hydraulic Research, (1986). Vol. 24(4), pp. 265-280.
[18] Tiedeman, S.A., Allsop, W., Russo, V., and Brown, A. A demountable wave absorber for wave flumes and basins. Coastal Engineering Proceedings, (2012), 1(33), 37. 1-10.
[19] Dean R., and Dalrymple R. Water wave mechanics for engineers and scientists, Singapore, Prentice Hall, 1991.
[20] Beneduce, M. (2019). Design of a wavemaker for the water tank at the Politecnico di Torino (Doctoral dissertation, Politecnico di Torino).
[21] Le Méhauté, B. An introduction to hydrodynamics and water waves. Springer Science & Business Media (2013).
[22] Sorensen, R.M. Basic Wave Mechanics for Coastal and Ocean Engineers. New York: John Wiley & Sons, Inc (1993).
[23] Liu, Y., Cavalier, G., Pastor, J., Viera, R.J., Guillory, C., Judice, K., Guiberteaun K.,and Kozman, T.A. Design and construction of a wave generation system to model ocean conditions in the Gulf of Mexico. International Journal of Energy Technology, (2012). Vol. 4, pp. 1-7.
[24] Qin, S., Fan, J., Zhang, H., Su, J., & Wang, Y. Flume Experiments on Energy Conversion Behavior for Oscillating Buoy Devices Interacting with Different Wave Types. Journal of Marine Science and Engineering, (2021), 9(8), 852.
[25] Saincher, S., and Banerjeea, J. Design of a mumerical wave tank and wave flume for low steepness waves in deep and intermediate water. Procedia Engineering, (2015). Vol. 116, pp. 221–228.
[26] Hughes S.A. Physical models and laboratory techniques in coastal engineering, Singapore, World Scientific Publishing, 1993.
[27] Izquierdo, U., Galera-Calero, L., Albaina, I., Vazquez, A., Esteban, G.A., & Blanco, J.M. Experimental and numerical determination of the optimum configuration of a parabolic wave extinction system for flumes. Ocean Engineering, (2021), 238, 109748.